

This document is confidential and is proprietary to the American Chemical Society and its authors. Do not copy or disclose without written permission. If you have received this item in error, notify the sender and delete all copies.

The structural basis of small molecule targetability of monomeric Tau protein

Journal:	<i>ACS Chemical Neuroscience</i>
Manuscript ID	cn-2018-00182p.R1
Manuscript Type:	Article
Date Submitted by the Author:	n/a
Complete List of Authors:	Kiss, Róbert; Hungarian Academy of Sciences, Research Centre for Natural Sciences Csizmadia, Georgina ; Research Center for Natural Sciences, Hungarian Academy of Sciences Solti, Katalin; Research Center for Natural Sciences, Hungarian Academy of Sciences Keresztes, Attila; Biological Research Center, Hungarian Academy of Sciences, Biochemistry Zhu, Max; Cantabio Pharmaceuticals Pickhardt, Marcus; DZNE (German Center for Neurodegenerative Diseases), Mandelkow, Eckhard; Deutsches Zentrum für Neurodegenerative Erkrankungen Toth, Gergely; University of Cambridge, Chemistry

SCHOLARONE™
Manuscripts

The structural basis of small molecule targetability of monomeric Tau protein

Róbert Kiss,¹ Georgina Csizmadia,^{1†} Katalin Solti,¹ Attila Keresztes,^{1¶} Max Zhu,² Marcus Pickhardt,^{3,4} Eckhard Mandelkow,^{3,4} Gergely Tóth^{1,2*}

¹ MTA-TTK-NAP B - Drug Discovery Research Group – Neurodegenerative Diseases, Institute of Organic Chemistry, Research Center for Natural Sciences, Hungarian Academy of Sciences, Budapest, Hungary

² Cantabio Pharmaceuticals, Sunnyvale, California, USA

³ Deutsches Zentrum für Neurodegenerative Erkrankungen (DZNE), Sigmund-Freud-Str. 27, 53127 Bonn, Germany

⁴ CAESAR Research Center/ Max-Planck-Institute, Ludwig-Erhard-Allee 2, 53175 Bonn, Germany

*corresponding author: toth.gergely@ttk.mta.hu or gtoth@cantabio.com

KEYWORDS: *Tau, intrinsically disordered, modeling, conformational ensemble, methylene-blue, binding site, structure-based, drug design*

ABSTRACT

1
2
3 The therapeutic targeting of intrinsically disordered proteins (IDPs) by small molecules has been a chal-
4 lenge due to their heterogeneous conformational ensembles. A potential therapeutic strategy to alleviate
5 the aggregation of IDPs is to maintain them in their native monomeric state by small molecule binding.
6 This study investigates the structural basis of small molecule druggability of native monomeric Tau
7 whose aggregation is linked to the onset of Tauopathies such as Alzheimer's disease. Initially, two avail-
8 able monomeric conformational ensembles of a shorter Tau construct K18 (also termed Tau4RD) were
9 analyzed which revealed striking structural differences between the two ensembles, while similar num-
10 ber of hot spots and small molecule binding sites were identified on monomeric Tau ensembles as on
11 tertiary folded proteins of similar size. Remarkably, some critical fibril forming sequence regions of Tau
12 (V306-K311, V275-K280) participated in hot spot formation with higher frequency compared to other
13 regions. As an example of small molecule binding to monomeric Tau, it was shown that methylene blue
14 (MB) bound to monomeric K18 and full-length Tau selectively with high affinity ($K_d = 125.8$ nM and
15 86.6 nM, respectively) with binding modes involving Cys291 and Cys322, previously reported to be
16 oxidized in the presence of MB. Overall, our results provide structure-based evidence that Tau can be a
17 viable drug target for small molecules and indicate that specific small molecules may be able to bind to
18 monomeric Tau and influence the way in which the protein interacts among itself and with other pro-
19 teins.
20
21
22
23
24
25
26
27
28
29
30
31
32
33
34
35
36
37
38
39
40
41
42
43
44
45
46
47
48
49
50
51
52
53
54
55
56
57
58
59
60

INTRODUCTION

Tauopathies¹ are a subset of neurodegenerative disorders, including Alzheimer's disease (AD)² and frontotemporal dementias (FTD)³, which are linked to the accumulation of neurofibrillary tangles (NFTs) that are formed by the aggregation of microtubule associated protein Tau (MAPT) in patients' brain cells. The aggregation of monomeric Tau in neurons leads to the instability of microtubules in the axons, and the presence of Tau oligomers and fibrils generated through its aggregation cause toxic effects in neurons resulting in neurodegeneration.

Intrinsically disordered proteins (IDP) such as the Tau protein have been considered as intractable drug targets for small molecule drug discovery due to the lack of a stable 3D structure. Therefore Tau has been neglected by most small molecule drug discovery programs and has been mostly targeted by specific monoclonal antibodies for immunotherapy⁴⁻⁵. Since Tau is an intra-cellular protein localized mostly in neurons, it is not clear whether antibody-based drug development efforts will lead to efficacious treatments. Moreover, the economic cost of a potential immunotherapy for tens of millions of patients with Tauopathies will not likely be affordable for our society. Therefore, it is critical to explore alternative small molecule approaches targeting the Tau protein for the development of disease modifying therapeutics.

The soluble monomeric state of Tau has been studied by NMR spectroscopy⁶⁻⁹, which showed that the structure of monomeric Tau is made up of a diverse conformational ensemble. This conformational ensemble is not completely random: some pronounced intramolecular interactions exist and some regions have some propensity to adopt defined secondary structure⁶⁻⁹.

Computational structure-based modeling approaches are applied to generate conformational ensembles of IDPs, which use experimentally derived observations such as NMR, small-angle X-ray and FRET experimental data¹⁰. Two main approaches exist for generating conformational ensembles, the so-called pool-based and the molecular dynamics (MD) based approach. Typically, the extent and resolution of the experimental data is not sufficient for either approach to generate accurate high resolution 3D structures. Recently, two conformational ensembles of the monomeric form of Tau have been published^{6, 11}.

We have previously explored whether small molecule binding pockets can exist within members of the heterogeneous conformational ensemble of IDPs despite their overall lack of persistent structures. Our results from investigating monomeric α -synuclein¹² and A β 42 peptide¹³ suggest that locally persistent binding sites are present even within a diverse population of conformations of these proteins. Moreover,

1 a recent analysis of publicly available conformational ensembles of some IDPs found that IDPs have a
2 comparable number of potential binding sites as proteins with ordered 3D tertiary structure¹⁴.
3

4 Binding of small molecules to such pockets may have distinct effects such as altering the conforma-
5 tional ensemble of IDPs and possibly impacting the dynamics and thermodynamic stability of the vari-
6 ous conformational states¹². The basis of the binding mechanism of small molecules to IDPs is yet to be
7 clearly elucidated, nevertheless it has been assumed that it involves conformational selection by the
8 binding ligand^{12-13, 15}. Consequently, targeting the conformational ensemble of the apo form of IDPs
9 could be a viable structure-based drug discovery strategy. We previously successfully applied this ap-
10 proach for the basis of a structure-based computational docking screen on the conformational ensemble
11 of α -synuclein to identify novel fragment and drug-like small molecules targeting monomeric α -
12 synuclein, one of which was active in cellular models of α -synuclein-mediated dysfunction¹². In another
13 recent study, novel compounds binding to c-Myc were identified by structure-based virtual screening on
14 three binding pockets of representative c-Myc conformations¹⁶.
15
16
17
18
19
20
21
22

23 Only a limited number of small molecule ligands of monomeric Tau have been described in the litera-
24 ture¹⁷⁻¹⁸. Most of the identified compounds are, however, suboptimal for further drug discovery optimi-
25 zation, as they have either non-druglike physicochemical properties or contain reactive functional
26 groups that are frequently associated with toxicity issues and lack of specificity¹⁹⁻²¹. Recently, we ap-
27 plied a unique biophysics based binding screening methodology to detect the binding between small
28 molecules and monomeric Tau, which led to the identification of a diverse set of novel fragment and
29 lead-like small molecules capable of interacting with Tau, some of which were able to reduce the aggre-
30 gation of Tau *in vitro* and in a cellular model of Tauopathies²². The study demonstrates that monomeric
31 Tau can be a viable receptor of small drug-like molecules, and supports the potential and practical feasi-
32 bility of the therapeutic strategy to target early phases of the aggregation pathway of Tau and potentially
33 other IDPs by small molecules, thereby eliminating the formation of potential toxic misfolded protein
34 species. This and other studies suggest that the structure-based identification of novel small molecules
35 binding to IDPs, such as monomer Tau, could be a viable drug discovery strategy²³.
36
37
38
39
40
41
42
43
44
45

46 One of the most studied Tau interacting ligand is methylene blue (MB) (Fig. S1), an approved treat-
47 ment for methemoglobinemia, which has been shown to have a wide range of interacting protein part-
48 ners and biological activities²⁴. MB was shown to inhibit Tau aggregation²⁵ and to disintegrate Tau fi-
49 brillar aggregates. In particular, Taniguchi *et al.* showed that MB inhibits heparin-induced Tau filament
50 formation ($IC_{50} = 1.9 \mu M$)²⁶. Thionine (a desmethyl derivative of MB) showed inhibition of Tau-Tau
51 binding ($IC_{50} = 98 nM$)²⁵. MB also promoted the oxidation of the cysteine residues of Tau (C291 and
52 C322), to sulfenic (SO), sulfinic (SO₂) and sulfonic (SO₃) forms, *in vitro*, and thus presumably inhibit
53
54
55
56
57
58
59
60

1 the aggregation of the protein by retaining it in an oxidized monomeric conformation²⁷⁻²⁸. Interestingly,
2 MB also inhibited caspase 1 and 3 activities *in vitro* through the oxidization of their catalytic cysteine²⁹.
3 Moreover, MB protected from Tau over-expression caused neurotoxicity *in vivo*³⁰⁻³¹ and MB based ther-
4 apeutic candidate, LMTX[®] (TauRx's second-generation Tau aggregation inhibitor (TAI)), has been
5 through several phase 3 clinical trials in AD and is still under investigation in further phase 3 clinical
6 trials in AD.
7
8
9

10 We set out to continue to investigate the small molecule targetability of IDPs, by focusing on Tau pro-
11 tein. Small molecules may have the potential to bind to specific conformations of monomeric Tau that
12 could influence the way in which Tau interacts among itself and with other proteins in neurons. Thus,
13 binding small molecules to monomeric Tau could alter its aggregation propensity, or perturb the mal-
14 function or the toxicity in neurons caused by Tau aggregation, or influence Tau modulated signal trans-
15 duction. In this study, we characterized the structural diversity and availability of small molecule bind-
16 ing sites within two published conformational ensembles of Tau and analyzed their applicability to ra-
17 tional drug design. Moreover, we investigated binding ability of MB to monomeric Tau as a model sys-
18 tem for Tau interactions using computational structure based and biophysical experimental approaches.
19 Our results yield further insights on the applicability of available IDP conformational ensembles, exist-
20 ence of binding sites, and provide a better understanding of the targetability of monomeric Tau by small
21 molecules.
22
23
24
25
26
27
28
29
30
31
32
33

34 RESULTS

35 Characterization of monomeric Tau ensembles

36 The two publicly available 3D structural ensembles of monomeric K18 Tau, comprising the repeat
37 domain responsible for aggregation, were collected and analyzed to assess their structural diversity and
38 their potential applicability for structure-based drug discovery. Ensemble 1 (ENS#1) was reported by
39 Ozenne *et. al.*⁶ consisting of 801 Tau conformers at high resolution, and the second ensemble 2 (ENS#2)
40 was reported by Fisher *et. al.*¹¹ containing 75 conformers.
41
42
43
44
45
46

47 Both Tau ensembles were found to be substantially diverse because the closest internal conformers
48 had a root-mean-square deviation (RMSD) of 11.28 Å (ENS#1) and 9.26 Å (ENS#2), respectively. The
49 overall diversity of the individual ensembles was similar when all RMSD matrix elements were consid-
50 ered (average RMSD) (Fig. 1A), while the minimum RMSD of each conformer to its closest neighbor
51 (minimum RMSD) was larger for ENS#2 (Fig. 1B), which may be attributed to the lower ensemble size
52 of ENS#2.
53
54
55
56
57
58
59
60

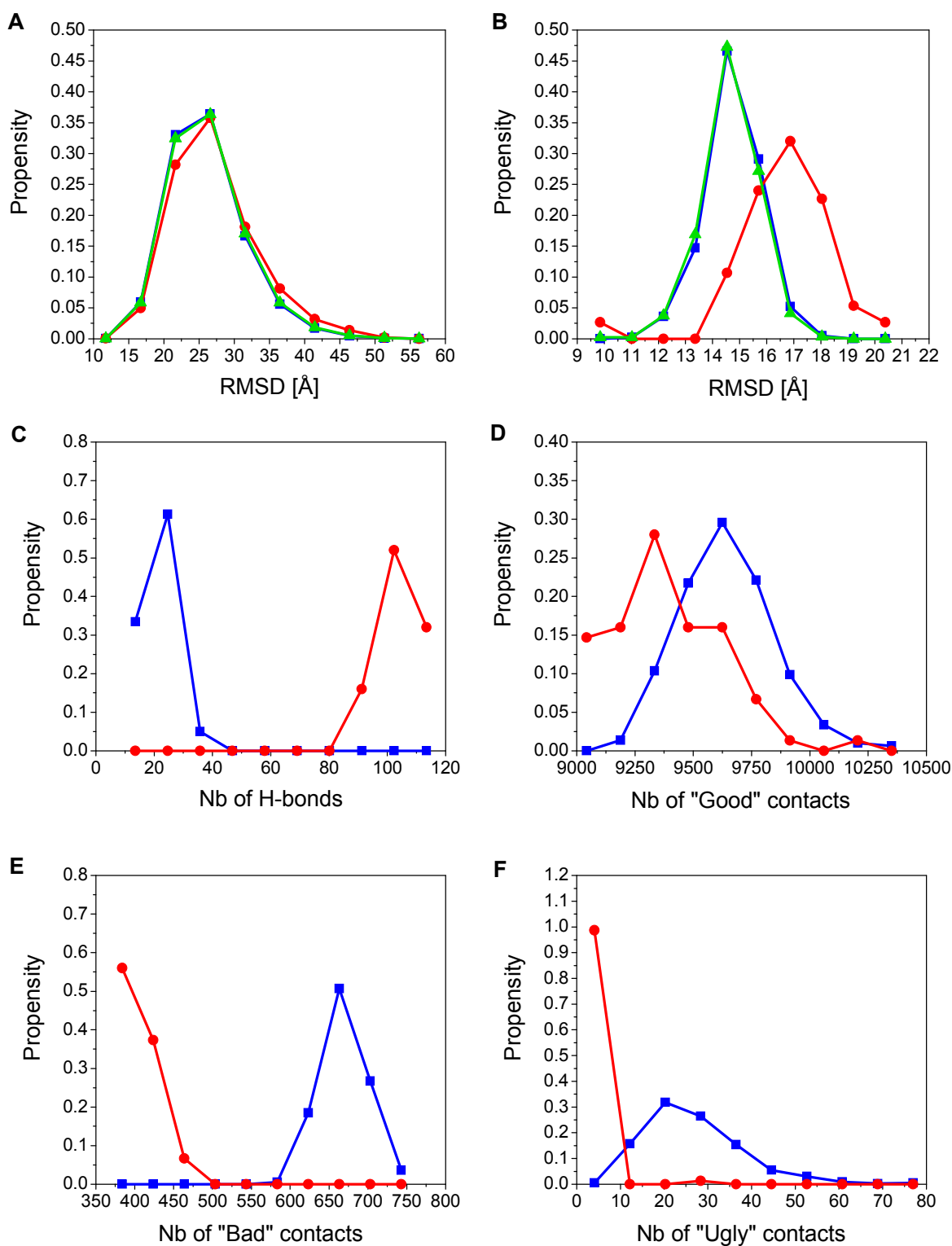


Figure 1. RMSD distribution curves of monomeric Tau ensembles ENS#1 (blue), ENS#2 (red) and the combined ensemble (green) calculated for all RMSD matrix elements (average RMSD) (A) and between each conformer and their closest conformer (minimum RMSD) (B). Distribution of the number (Nb) of intramolecular contacts in monomeric Tau ensembles ENS#1 (blue) and ENS#2 (red): number of H-

bonds (C), number of “Good” contacts (D), number of “Bad” (E) and number of “Ugly” (F) contacts (see definitions in Methods).

Surprisingly, when the two ensembles were combined, the closest conformers in the combined set had an RMSD of 9.26 Å (as in ENS#2) exposing that the two ensembles contain significantly different conformations. (The full RMSD matrices are shown in Fig. S2). To assess the compactness of the conformers, intramolecular contacts were calculated. Interestingly, many more van der Waals contacts (“Good”, “Bad” and “Ugly” – see definitions in Methods) were found in ENS#1, while ENS#2 contained more H-bonds (Fig. 1C-F). To further assess the compactness of the ensembles, the radii of gyration (Rg) of the conformers were calculated. ENS#1 had lower Rg value distribution in line with the higher number of van der Waals contacts (Fig. S3). The secondary structural content of the conformers was calculated, which indicated that some regions show higher propensity of helical and β -sheet secondary structures (Fig. 2A and 2B).

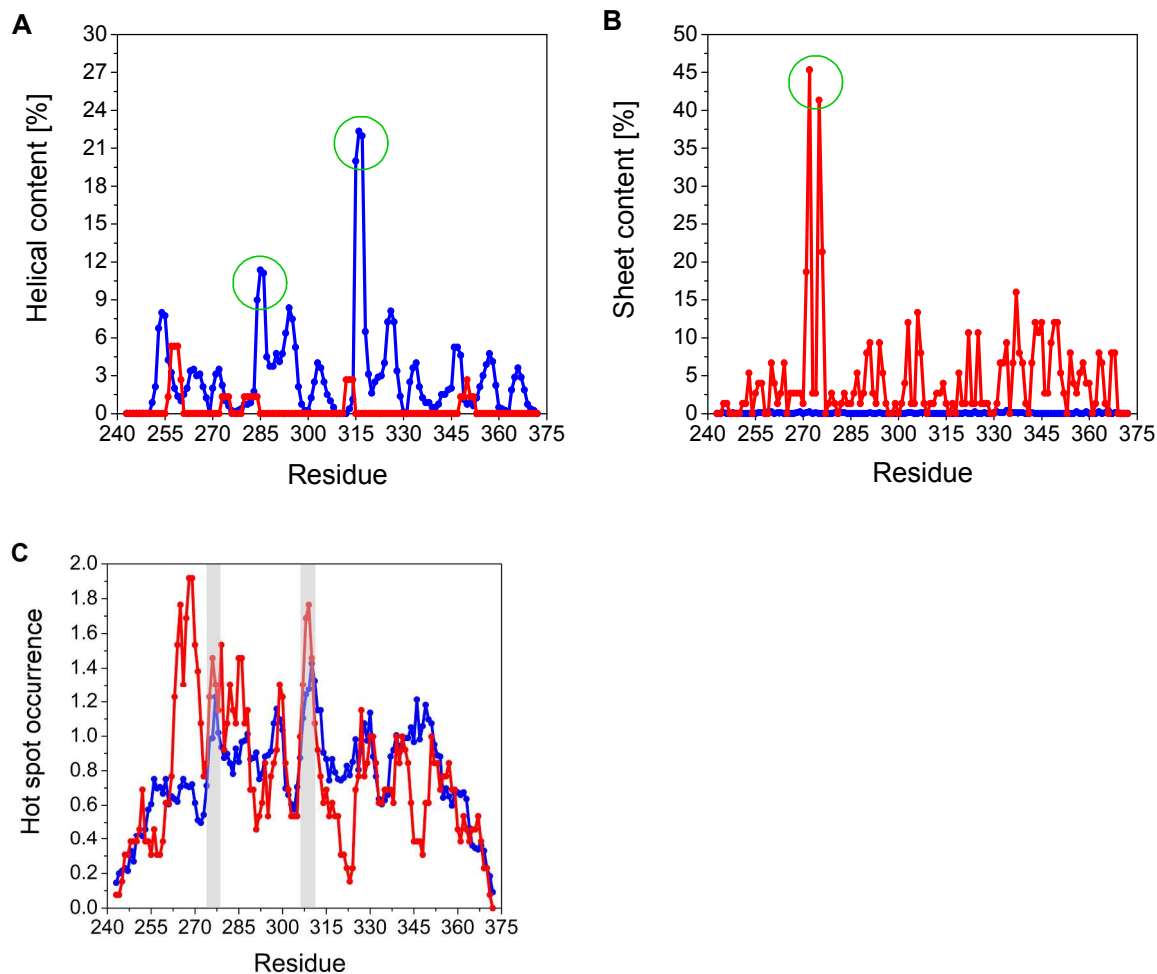
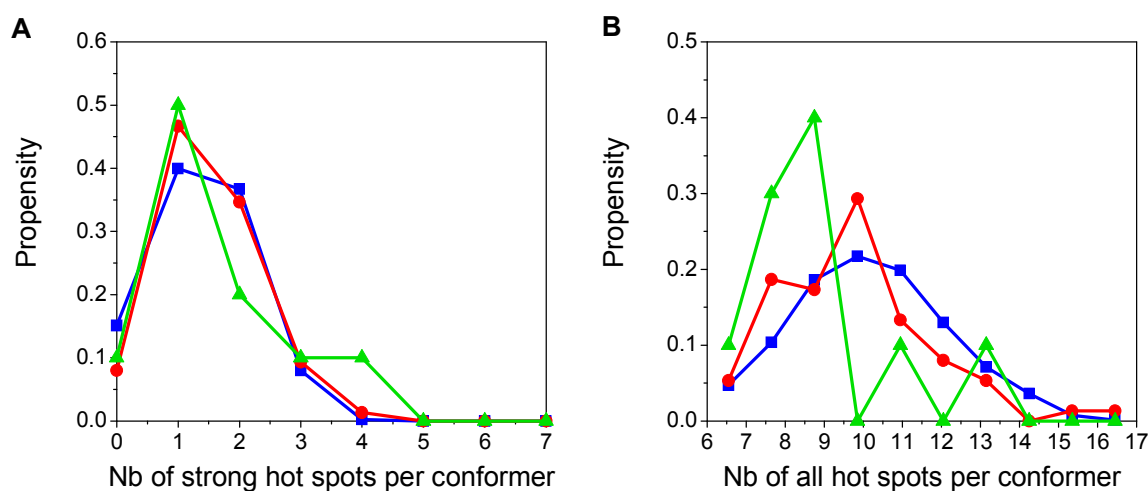


Figure 2. Distribution of helical (A) and β -sheet (B) secondary structure content in monomeric Tau ensembles ENS#1 (blue) and ENS#2 (red). Regions of higher secondary structure propensity are marked by green circles. Hot spot formation propensity (C) of residues in monomeric Tau ensembles ENS#1 (blue) and ENS#2 (red). Fibril-forming regions (V306-K311 and V275-K280) are indicated by larger markers / dashed lines.

In particular, the secondary structure analysis suggested higher propensity for nascent helices between residues L284-N286 and L315-K317 and increased propensity for β -structured conformation between residues G271-Q276. This latter region coincides with the V275-K280 sequence that has been shown to play a critical role in forming the core of Tau fibrils³²⁻³⁴. Moreover, the P270-G273 region has been suggested to form a β -hairpin conformation³⁵. Unexpectedly, the two ensembles feature completely different secondary structure elements: helical structures were solely found in ENS#1, while β structures were only present in ENS#2 (Fig. 2A and 2B).

Small molecule binding site mapping

Next, all Tau conformers were mapped for the presence of potential hot spots and small molecule binding sites using FTMap³⁶. The mapping results revealed that the intrinsically disordered monomeric state of Tau contained similar number of binding hot spots (Fig. 3A and 3B) and binding sites (Fig. 3C) as the investigated folded proteins with tertiary structure.



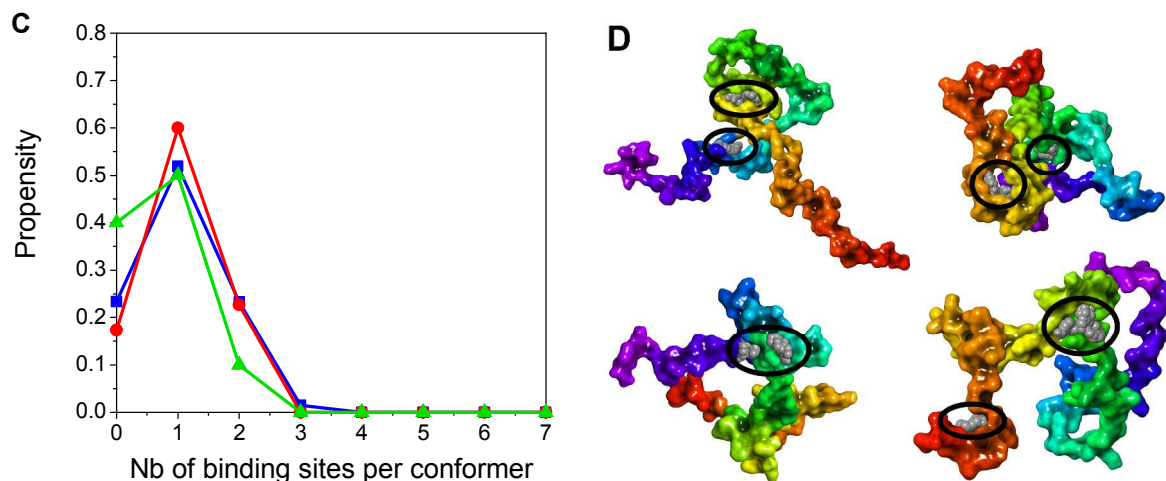


Figure 3. Distribution of the number (Nb) of strong binding hot spots (A), number (Nb) of all binding hot spots (B) and binding sites (C) in monomeric Tau ensembles ENS#1 (blue) and ENS#2 (red) and folded proteins (green) (see definitions of strong hot spots and binding sites in Methods). Binding hot spot examples (black circles) on selected Tau conformations (D).

In particular, the distribution of strong hot spots (see definition in Methods) that are essential for binding site formation was almost identical for ENS#1 and ENS#2 as for folded proteins (Fig. 3A). Moreover, the Tau ensembles contained more weak hot spots and an approximately similar number of binding sites compared to folded tertiary proteins (Fig. 3). Solvent accessible surface area (SASA) of the hot spots showed similar distribution for ENS#1 and ENS#2 (Fig. S4).

The tendency of individual residues to form binding hot spots was also analyzed. The two most critical fibril forming regions of Tau, the hexapeptide motifs V306-K311, V275-K280, are among the most frequently occurring residues in forming the hot spots (Fig. 2C). In particular, the V306-K311 region formed hot spots with highest propensity in ENS#1 and second highest in ENS#2. These results suggest that the monomeric structural ensembles of Tau investigated contain hot spots and targetable small molecule binding sites, which indicates that intrinsically disordered Tau may be a tractable target for small molecule drug discovery.

Investigation of the monomeric Tau binding characteristics of methylene blue

To elucidate further the interaction between MB with Tau, we investigated whether MB can oxidize cysteines in general by using glutathione (GSH), as standard model molecule generally used in covalent drug discovery³⁷ with the aim to gain insights into the thiol oxidation reactivity of MB. Our experiments

showed that MB does not form any covalent complexes with GSH, however, it facilitates the oxidation of GSH (Fig. 4A).

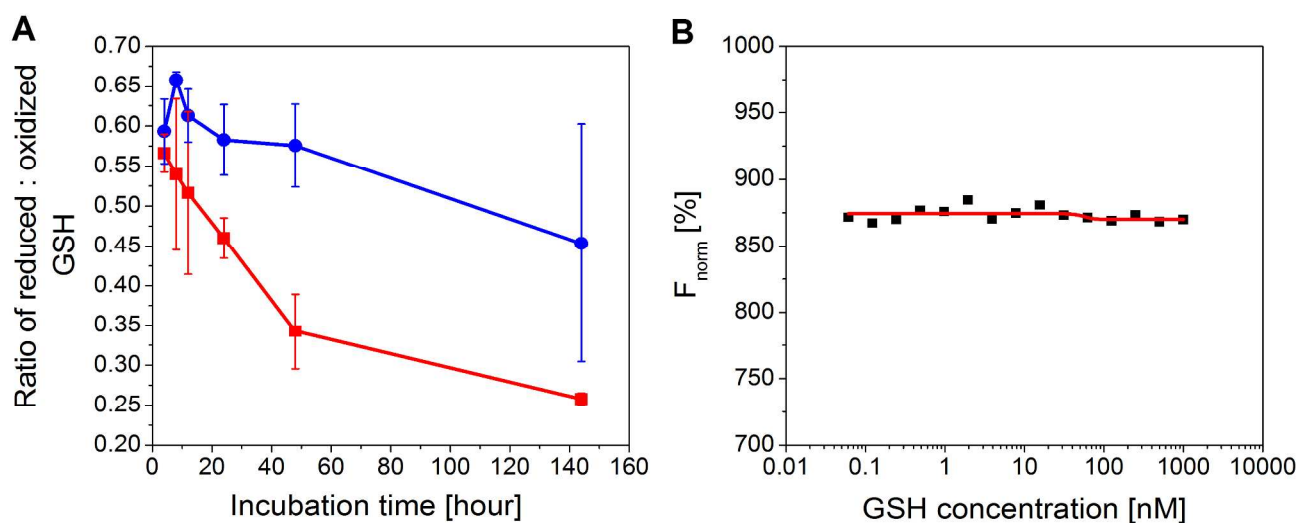


Figure 4. Oxidation kinetics of glutathione (GSH) in the presence (red) and absence (blue) of methylene blue (MB) monitored by LC-MS (A). Standard deviation is indicated by error bars. Dose-response curve between GSH and MB based on measured microscale-thermophoresis shows that no direct interaction could be detected (B). The fluorescence of MB was exploited for the MST experiments.

Given that GSH is a small flexible peptide, it is unlikely that MB has a specific affinity to GSH driven by non-bonded interactions. To elucidate this we tested whether GSH binds to MB using microscale thermophoresis (MST). The strong fluorescence properties of MB (Exc_{max} : 665 nm; Em_{max} : 692 nm) enables its label-free application as a sensitive molecular interaction detection system in MST. The MST experiments showed no sign of the existence of detectable interaction between MB and GSH (Fig. 4B). This suggests that the oxidation of GSH by MB was driven by diffusional effects.

Next, this MST set-up was further applied to characterize the affinity of MB to monomeric Tau. The concentration-dependent change in thermophoresis and T-jump signals indicated that MB binds both to monomeric full-length (Fig. 5A) and to monomeric K18 Tau with K_d values of 86.6 ± 8.8 nM and 125.8 ± 5.4 nM (Fig. 5B), respectively, whereas MB bound only weakly to BSA ($K_d > 1$ μ M) (Fig. 5C).

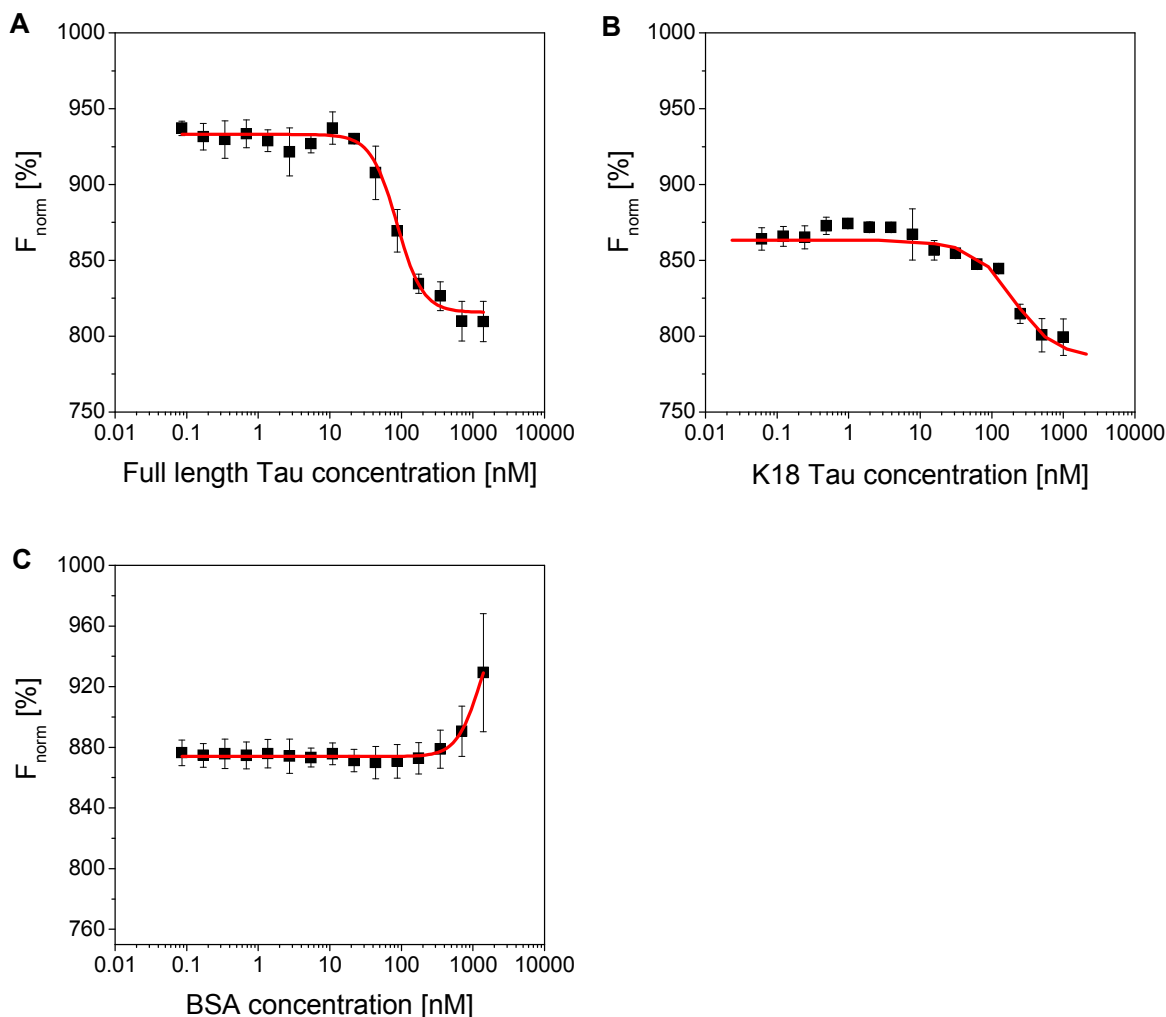


Figure 5. Dose-response curve between MB and monomeric full-length Tau (A), K18 Tau (B) and bovine serum albumin (C) based on measured combined T_{jump} and microscale thermophoresis data.

Overall, these results suggest that MB binds to monomeric Tau with reasonably high affinity and with some specificity, and this binding is non-covalent by nature. Consequently, MB herein will be used as a model ligand to evaluate the targetability of monomeric Tau ensembles by structure-based docking of small molecules.

Exploration of the binding site of methylene blue to monomeric Tau

To identify the potential binding sites of MB to monomeric Tau, we applied structure-based docking calculations to each of the predicted small molecule binding sites of the Tau conformations from both ensembles. All possible binding modes of MB generated by the docking program FRED were rank ordered by a consensus scoring scheme (see Methods for details), which provided a rank of the predicted binding modes of MB to Tau. The distribution of the consensus ranks is plotted in Fig. 6.

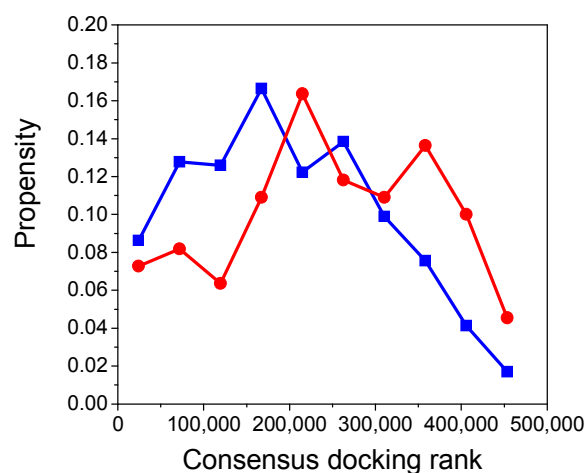
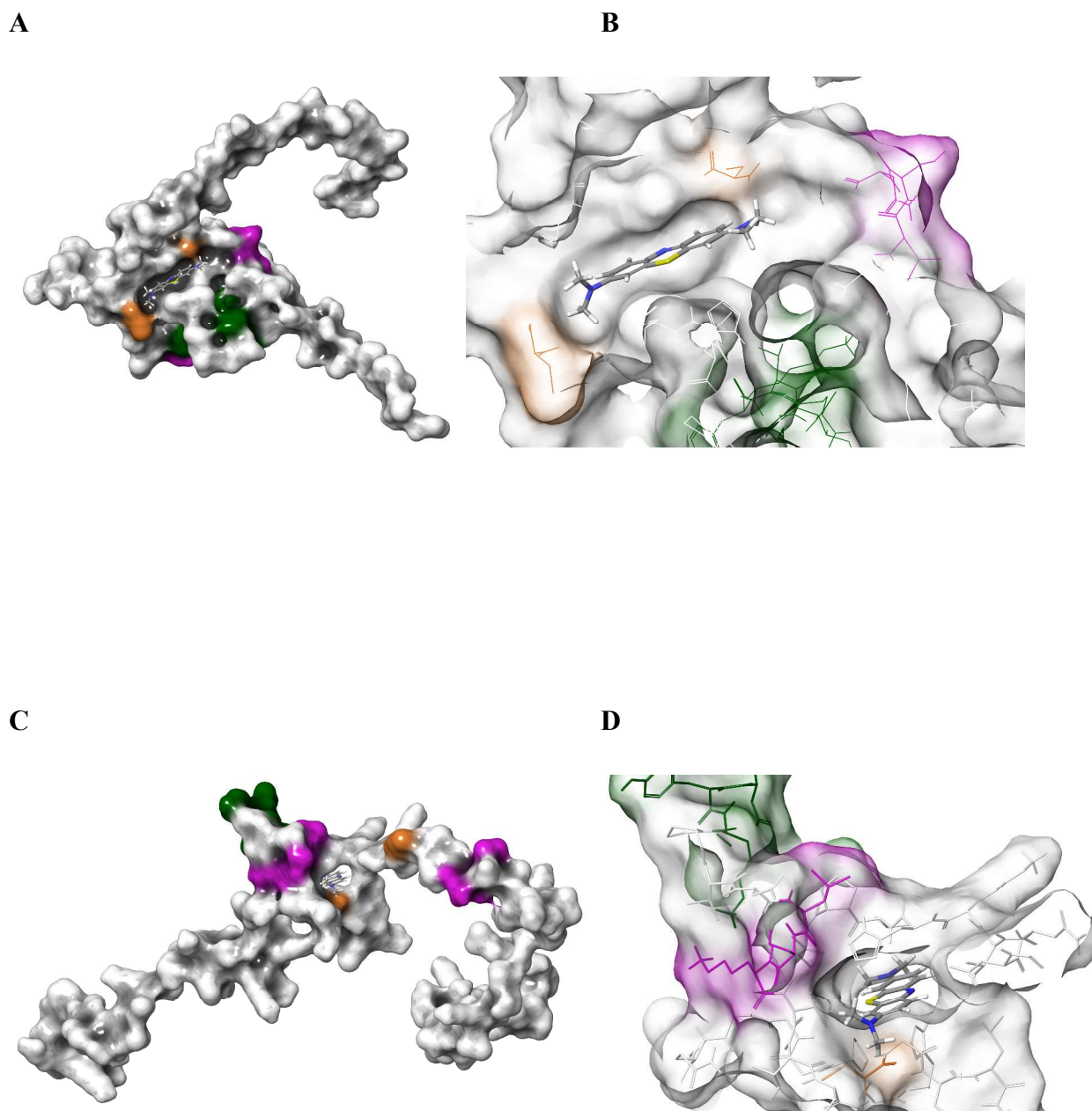


Figure 6. Distributions of the ranks of MB binding modes to the binding sites of monomeric Tau ensembles ENS#1 (blue) and ENS#2 (red).

Several potential binding modes of MB at different binding sites of monomeric Tau were identified in both Tau ensembles. The docking results indicated more favorable binding of MB to Tau conformations in ENS#1 compared to ENS#2 (Fig. 6). Binding conformations in close proximity of C291 and C322 were selected as these residues were suggested to be directly involved in MB binding on the basis of NMR HSQC measurements and the oxidation of both cysteine residues due to MB²⁸. 206 MB binding poses were identified, where either C291 or C322 was found within 6 Å proximity of MB. Out of these 206 binding poses, 9 (8.0% hit rate) belonged to ENS#1 and 197 (17.7% hit rate) to ENS#2, respectively (Fig. S5).

These MB binding modes were ranked by the consensus docking ranks and the highest ranked 10% (21) of the poses were selected for further analysis. In the 21 selected poses ENS#2 was over-represented: 20 poses (1.8%) from ENS#2 compared to 1 pose (0.9%) from ENS#1. In one of the 21 finally selected docking poses MB was found within 6 Å from both C291 and C322 (Fig. 7A and 7B).



41 **Figure 7.** Predicted binding poses of MB in selected representative conformations of K18 of Tau. Bind-
42 ing pose #4 (A, B): MB is in close proximity to both C291 and C322. Binding pose #1 (C, D): highest
43 ranked binding pose of MB by consensus scoring (Coloring scheme is the following: C291 and C322 in
44 orange, fibril forming region V306-K311 in green and nascent helical regions L284-N286 and L315-
45 K317 in magenta).
46
47
48
49

50
51
52 The highest ranked binding mode of MB is shown in Fig. 7C and 7D. In both binding modes the fibril
53 forming V306-K311 region as well as the nascent helical regions (L284-N286 and L315-K317) contrib-
54 uted to binding site formation. All interacting residues are listed in Table S1.
55
56
57
58
59
60

1 In summary, we identified potential binding sites and modes of MB to Tau, using previous experi-
2 mental results²⁸ demonstrating that structure-based modeling can be applied on conformational ensem-
3 bles of monomeric Tau. This suggests that such approach may be also useful for the development of
4 Tau targeting small molecule therapeutic candidates.
5
6
7
8
9

10 DISCUSSION AND CONCLUSION

11 Comparison of two distinct monomer Tau conformational ensembles

12 While both Tau conformational ensembles analyzed satisfy the global experimental parameters of
13 monomeric Tau according to their authors, striking structural differences were identified between the
14 two ensembles. In particular, the closest conformers between ENS#1 and ENS#2 were more dissimilar
15 than the closest conformers in ENS#2 (RMSD = 9.26 Å). In other words, the conformations of the two
16 ensembles had significantly different RMSD at the global level, although this does not exclude the pos-
17 sibility of local similarities. In line with the RMSD differences, the internal contact profiles of the two
18 ensembles also differed substantially. Moreover, nascent helical and β -sheet structures were unevenly
19 distributed in the two ensembles: helical structures were solely found in ENS#1, while β -sheet struc-
20 tured conformations were only captured by ENS#2.
21
22
23
24
25
26
27
28
29

30 Plausible explanations for these striking differences in the two ensembles may be the followings. The
31 level of disorder in monomeric Tau has been particularly high and the acquisition of relevant experi-
32 mental data that can be translated to structural constraints is limited in extent and resolution. Therefore
33 multiple possible conformational ensembles can be generated that satisfy the limited number of experi-
34 mental constraints. The sampling of both reported ensembles may be insufficient, as they are selected to
35 satisfy all constraints by the smallest possible set of conformers. In addition, more, relevant experi-
36 mental data that can be translated to local structural constraints and utilized during ensemble generation
37 are needed. In particular, it has been suggested that novel techniques capable of sampling proteins on a
38 longer timescale would be required for a better characterization of IDPs³⁸.
39
40
41
42
43
44
45

46 Nevertheless, in both cases, the individual conformations of the published ensembles may represent
47 relevant, energetically favored conformations of monomeric Tau that can be targeted by structure-based
48 drug discovery. The results of this study suggest that the folding of different segments of Tau is required
49 for the formation of the binding site and the complete monomeric Tau structure is not required for ac-
50 commodating small molecule ligands. We also made similar observation when studying the conforma-
51 tional ensemble of intrinsically disordered α -synuclein¹² and A β 42¹³. Similarly to the α -synuclein
52 study¹², we identified similar number of hot spots and binding sites on the ensembles compared to ran-
53
54
55
56
57
58
59
60

domly selected folded proteins possessing tertiary structure suggesting that it is feasible to identify high affinity ligands to Tau and that this may be a general character of IDPs.

Remarkably, we found that some critical fibril forming regions (V306-K311, V275-K280) of Tau participated in hot spot formation with higher frequency compared to other sequence regions. These regions may be particularly relevant when targeting Tau with small molecules as they could potentially block fibril formation by competing with other Tau interacting surfaces that are critical for aggregation.

On the binding mechanism of MB to Tau

To demonstrate the applicability of the available conformational ensembles of Tau for structure-based drug discovery, we selected MB and predicted its potential binding mode to Tau. To establish the MB – Tau complex as a validated model system for this study, we further explored its mechanism of interaction between MB and monomeric Tau *in vitro*. MB has been shown to bind to monomeric Tau previously²⁸.

The interaction of MB with monomeric Tau is complex. MB has been shown to be able to oxidize cysteine residues of monomeric Tau²⁷⁻²⁸. However, this is likely a non-specific event, as we show that MB can oxidize solvent accessible cysteines on a small molecule as GSH. Nevertheless, we observed concentration-dependent change in thermophoresis of MB when either full-length or K18 Tau was administered. In contrast, no such changes were observed in the thermophoresis of MB when GSH was administered to it instead of Tau. This suggests that MB binds to monomeric Tau reversibly via non-bonded interactions. The docking simulations of MB revealed potential binding modes that are in reasonably good agreement with the available experimental data. In particular MB was found to bind in close proximity of C291 / C322 which were shown to be oxidized during MB administration²⁸.

Small molecule binding sites exist on monomeric Tau

Our study of monomeric Tau structural conformational ensembles supports the results of our previous theoretical studies on α -synuclein¹² and A β 42¹³ ensembles in regard to the existence of small molecule binding sites on these IDPs. Our results in this study on the mechanism of binding of MB to Tau provide further experimental and theoretical evidence for the existence of binding sites on Tau. Additional evidence of this was demonstrated by our previous study²² in which we applied a biophysics-based high throughput screen to identify small molecule binders to monomeric full length Tau. A diverse set of novel fragment and lead-like small molecules were capable of binding monomeric Tau, some of which had also the ability to inhibit Tau aggregation. Overall, these results demonstrate that despite its heterogeneous conformational ensemble and a lack of stable tertiary structure, Tau can be a viable receptor for

1 small drug-like molecules. These findings have strong relevance to other IDPs in general and imply that
2 other IDPs may also have the ability to interact with drug-like small molecules. Our results imply that
3 specific small molecules may exist that could bind to monomeric Tau and influence the way in which
4 Tau interacts among themselves and with other proteins in neurons. These small molecules therefore
5 could alter the aggregation propensity of Tau and/or perturb Tau mediated cellular signal transduction.
6
7
8
9

11 METHODS

13 Structural data sources

15 Conformational ensembles of monomeric K18 Tau were collected from the PED database
16 (<http://pedb.vib.be/>)³⁹ (ENS#1) and from the supplementary material of the research article of Fisher *et*
17 *al.* (<http://www.rle.mit.edu/cbg/data.htm>)¹¹ (ENS#2). Initial ENS#1 ensemble contained 995 structures.
18 After superposition and backbone RMSD calculations 194 duplicate structures were eliminated resulting
19 in 801 structures (referred as ENS#1 throughout the manuscript). ENS#2 contained 75 individual struc-
20 tures that represents conformations with at least 0.0005 calculated probability. All 75 structures were
21 found unique after superposition and backbone RMSD calculations.
22
23
24
25
26
27

28 X-ray structures of proteins with identical length of K18 Tau (130 residues), with a maximum 30%
29 sequence identity were selected from the PDB database [<http://www.rcsb.org>]. Ten (PDB IDs: 1KNM,
30 2NWD, 3FYM, 3RFE, 4ESP, 4HWM, 4PS6, 4XPX, 4YTK, 5C6S) out of the 53 resulting structures
31 were selected based on the resolution of the structures.
32
33
34
35

36 RMSD matrix calculations

37 Tau structures were superimposed by their C-alpha atoms and backbone RMSD matrices were calcu-
38 lated for both ensembles in Maestro⁴⁰ using Conformer Cluster.
39
40
41

42 Prediction of side chain conformations

43 Original version of ensemble ENS#1 lacked side chain conformations. RASP⁴¹ was used by default
44 parameters to calculate the missing side chains for ENS#1.
45
46
47
48

49 Molecular contacts calculation

50 Intramolecular contacts were calculated and classified in Maestro⁴⁰ as follows: H-bonds: H...A dis-
51 tance must be less than 2.8 Å, the D-H...A angle must be greater than 120°, and the H...A-B angle must
52 be greater than 90°.
53
54
55

56 Contacts are defined by a ratio given by the following formula:
57
58
59
60

$$C = D12 / (R1 + R2)$$

where D12 is the distance between atoms 1 and 2, and R1 and R2 are the van der Waals radii of atoms 1 and 2. The contacts are classified into “Good”, “Bad”, and “Ugly” based on this ratio. The default values are: Good: $1.30 > C > 0.89$; Bad: $0.89 > C > 0.75$; Ugly: $C < 0.75$.

Secondary structure calculation

Per residue secondary structure was determined for all conformations of monomeric Tau by DSSP (<http://swift.cmbi.ru.nl/gv/dssp>)⁴² with default parameters.

Binding site mapping

The FTMap web server³⁶ (<http://ftmap.bu.edu/>) was used to identify binding hot spots and binding sites on the Tau conformers and selected folded proteins. According to the authors' instructions⁴³ “strong hot spot” was defined as a hot spot with a cross-cluster population > 16 . Additionally, a “binding site” was defined as a minimum set of two hot spots (one of which is a strong hot spot) within 8 Å distance.

Solvent accessible surface area of each hot spot was calculated in Maestro⁴⁰ using Create Binding Site Surfaces panel including residues within 5 Å of a single cross-cluster (set of docked solvent molecules by FTMap).

Ligand preparation

3D conformations of methylene blue (MB) were calculated by OMEGA⁴⁴⁻⁴⁵ by applying more thorough settings than default (strictfrags (true), sampleHydrogens (true), ewindow (20.0), maxconfs (10,000), maxtime (600.0), rms (0.3)). QUACPAC⁴⁶ was used to calculate am1bcc charges for each conformer (option: am1bccsym).

Molecular docking

Tau conformations were prepared for docking by using the pdb2receptor function of OEDocking⁴⁷⁻⁵⁰. Binding sites were defined based on the cross-clusters (set of docked solvent molecules by FTMap). Docking was carried out by FRED⁵¹ applying special parameters allowing a more thorough sampling and optimization (exhaustive_scoring (chemgauss3), rstep (0.75), tstep (0.5), num_poses (10,000), clash_scale (0.75), opt (chemgauss3), hitlist_size (1,000,000), num_alt_poses (100), sort_by_top_consensus_pose (true). Consensus pose selection was carried out using the following scoring functions and weights: pose_select_weight_shapegauss 1, pose_select_weight_plp 1, pose_select_weight_chemgauss3 1, pose_select_weight_oechemscore 1, pose_select_weight_screenscore 1. Consensus scoring was applied by combining the following scoring functions: shapegauss, plp, chemgauss3, oechemscore, screenscore.

Tau Protein Preparation

The human Tau constructs were expressed in pNG2 vector, a derivative of pET-3a (Merck-Novagen, Darmstadt) in *E. coli* strain BL21(DE3) (Merck-Novagen, Darmstadt)⁵². The expressed protein was purified from bacterial extract by making use of the heat stability of Tau protein. The cell pellet was resuspended in the boiling-extraction buffer (50 mM MES, 500 mM NaCl, 1 mM MgCl₂, 1 mM EGTA, 5 mM DTT, pH 6.8) complemented with protease inhibitor cocktail (1 mM PMSF, 1 mM EDTA, 1 mM EGTA, 1 mM benzamidin, 1 μg/ml leupeptin, 1 μg/mL aprotinin, and 1 μg/ml pepstatin). The cells were disrupted with a French pressure cell and subsequently boiled for 20 min. The soluble extract was isolated by centrifugation, the supernatant was dialyzed against the cation exchange chromatography buffer A (20 mM MES, 50 mM NaCl, 1 mM EGTA, 1 mM MgCl₂, 2 mM DTT, 0.1 mM PMSF, pH 6.8) and loaded on cation exchange SP-Sepharose column (GE Healthcare). The protein was eluted by a linear gradient of cation exchange chromatography buffer B (20 mM MES, 1 M NaCl, 1 mM EGTA, 1 mM MgCl₂, 2 mM DTT, 0.1 mM PMSF, pH 6.8). The short Tau constructs representing Tau repeat domains Tau3RD (3 repeats; (M)Q244-S372 lacking V275-S305, comprising 99 residues) were subsequently concentrated and rebuffed in PBS (pH 7.4) on Amicon Ultra-15 device (Millipore, Bedford, MA). Protein concentration was determined by the Bradford assay and the purity of the proteins was analyzed by SDS-PAGE (17%).

Microscale thermophoresis

Interactions between methylene blue (MB) and K18 or full-length Tau as well as between MB and glutathione (GSH) were characterized by microscale thermophoresis (MST) on a Monolith NT.115 instrument from Nanotemper as follows. The concentration of the fluorescent MB was kept constant at 100 nM and the concentration of proteins was increased in the samples during the MST experiments from 0 to 1400 nM. The proteins were dissolved in 10 mM HEPES, 5 mM NaCl, 0.005 % Tween 20 buffer solutions at pH = 7.4. 5 μl of the respective samples were filled in MST capillaries by simple capillary forces. The following stages are recorded for each sample: fluorescence signal before turning the IR laser on, thermophoresis of molecules and back diffusion after switching the laser off. The signal was recorded in all capillaries at varying concentration of the non-fluorescent protein. Samples were incubated at 25 °C within the capillaries for 30 min prior to running measurements. Assays were conducted at 40 % IR-laser power and MST powers (corresponding to the excitation strength of the LED) of 20%. Any change of thermophoretic properties is observed as a change in fluorescence intensity. The thermophoresis signal is plotted against the ligand concentration to obtain a dose-response curve, from which the binding affinity (K_d) can be deduced.

LC-MS

Oxidation kinetics of glutathione (GSH) (Sigma, St. Louis, MO, USA) were measured by LC-MS as follows. GSH was dissolved in PBS buffer at a final concentration of 250 μ M. 4 mM Indoprofen (Sigma, St. Louis, MO, USA) was dissolved in MeCN and added as a control for UV detection. Reduced GSH was detected in the presence or absence of 5 mM MB after 4, 8, 12, 24, 48 and 144 hours of incubation. Eluent A contained 10 mM ammonium-formate dissolved in 95% distilled water and 5% MeCN. Eluent B contained 10 mM ammonium-formate dissolved in 20 % distilled water and 80 % MeCN. The gradient was changed from 0 % to 100 % B in 1 min then hold 100 % B for 2.5 min and changed gradually to 0 % B in 1.5 min and hold at 0 % for 0.5 min. The operating conditions were as follows: nebulizer gas: 1.5 L/min; drying gas: 15 L/min; temperature of desolvation lines: 300 $^{\circ}$ C; temperature of column: 30 $^{\circ}$ C; time of measurement: 5 min; ionization: DUIS; recorded m/z range: 50-1000; column: WATREX rs15.9e.s1003, Reprospher 100 C18, 5 μ m, 100x3 mm; instrument: Shimadzu LCMS-2020

Statistics

To assess the significance of the differences between the distributions we applied Kolmogorov-Smirnov test, which is a nonparametric test to compare two distributions with different sample sizes as well as two sample, independent Student t-tests. Statistical analysis was carried out by XLSTAT⁵³.

SUPPLEMENTARY INFORMATION (SI)

SI contains supplementary material on the structural characterization of Tau conformational ensembles and on the description of the binding sites of MB on monomeric Tau.

AUTHOR INFORMATION

Corresponding Author

* Gergely Tóth at toth.gergely@ttk.mta.hu

Present Addresses

† Semmelweis University Department of Biophysics and Radiation Biology, Budapest, Hungary

¶ University of Arizona, College of Medicine, Department of Pharmacology, Tucson, AZ, USA

Author Contributions

1
2 R. K. co-designed *in silico* modelling and LC-MS studies and co-performed them with G. Cs. K. S. and
3
4 A. K. performed all MST experiments. M. P. generated recombinant K18 and full length Tau. G. T. con-
5
6 ceived the study, co-designed research experiments, analysed data and contributed to writing the manu-
7
8 script. All other authors contributed to the analyses of the data and to writing the manuscript. All au-
9
10 thors have given approval to the final version of the manuscript.

Funding Sources

11
12
13
14
15 We thank the Hungarian Brain Research Program 2017-1.2.1-NKP-2017-00002 for its funding support.
16
17
18
19

Acknowledgment

20
21
22 We thank György M. Keserű for his support with molecular modeling. We also thank the Hungarian
23
24 NIF for providing the HPC computing facilities.
25
26
27

Competing financial interests

28
29
30 We have read the journal's policy and make the following statements on competing financial interests:
31
32 some of the authors are employees and/or shareholders of Cantabio Pharmaceuticals as designated by
33
34 Cantabio affiliation. This does not alter our adherence to all the Science policies on sharing data and
35
36 materials.
37
38
39

ABBREVIATIONS

40
41
42 ENS#1, ensemble 1; ENS#2, ensemble 2; MB, methylene-blue; AD, Alzheimer's disease; FTD, fronto-
43
44 temporal dementias; NFTs, neurofibrillary tangles; MAPT, microtubule associated protein Tau; IDP,
45
46 intrinsically disordered proteins; Rg, radii of gyration; MD molecular dynamics; MST, microscale ther-
47
48 mophoresis; LCMS, liquid chromatography-mass spectrometry; RMSD, root-mean-square deviation;
49
50 GSH, glutathione; BSA, bovine serum albumin.
51
52
53
54
55
56
57
58
59
60

REFERENCES

1. Vieira, M. N.; Forny-Germano, L.; Saraiva, L. M.; Sebollela, A.; Martinez, A. M.; Houzel, J. C.; De Felice, F. G.; Ferreira, S. T., Soluble oligomers from a non-disease related protein mimic Abeta-induced tau hyperphosphorylation and neurodegeneration. *J Neurochem* **2007**, *103* (2), 736-48.
2. Ballatore, C.; Lee, V. M.; Trojanowski, J. Q., Tau-mediated neurodegeneration in Alzheimer's disease and related disorders. *Nat Rev Neurosci* **2007**, *8* (9), 663-72.
3. Olney, N. T.; Spina, S.; Miller, B. L., Frontotemporal Dementia. *Neurol Clin* **2017**, *35* (2), 339-374.
4. Sigurdsson, E. M., Tau Immunotherapy. *Neurodegener Dis* **2016**, *16* (1-2), 34-8.
5. Coughlin, D.; Irwin, D. J., Emerging Diagnostic and Therapeutic Strategies for Tauopathies. *Curr Neurol Neurosci Rep* **2017**, *17* (9), 72.
6. Ozenne, V.; Schneider, R.; Yao, M.; Huang, J. R.; Salmon, L.; Zweckstetter, M.; Jensen, M. R.; Blackledge, M., Mapping the potential energy landscape of intrinsically disordered proteins at amino acid resolution. *J Am Chem Soc* **2012**, *134* (36), 15138-48.
7. Mukrasch, M. D.; Markwick, P.; Biernat, J.; Bergen, M.; Bernado, P.; Griesinger, C.; Mandelkow, E.; Zweckstetter, M.; Blackledge, M., Highly populated turn conformations in natively unfolded tau protein identified from residual dipolar couplings and molecular simulation. *J Am Chem Soc* **2007**, *129* (16), 5235-43.
8. Mukrasch, M. D.; Bibow, S.; Korukottu, J.; Jeganathan, S.; Biernat, J.; Griesinger, C.; Mandelkow, E.; Zweckstetter, M., Structural polymorphism of 441-residue tau at single residue resolution. *PLoS Biol* **2009**, *7* (2), e34.
9. Fischer, D.; Mukrasch, M. D.; von Bergen, M.; Klos-Witkowska, A.; Biernat, J.; Griesinger, C.; Mandelkow, E.; Zweckstetter, M., Structural and microtubule binding properties of tau mutants of frontotemporal dementias. *Biochemistry* **2007**, *46* (10), 2574-82.
10. Varadi, M.; Vranken, W.; Guharoy, M.; Tompa, P., Computational approaches for inferring the functions of intrinsically disordered proteins. *Front Mol Biosci* **2015**, *2*, 45.
11. Fisher, C. K.; Huang, A.; Stultz, C. M., Modeling intrinsically disordered proteins with bayesian statistics. *J Am Chem Soc* **2010**, *132* (42), 14919-27.
12. Toth, G.; Gardai, S. J.; Zago, W.; Bertocini, C. W.; Cremades, N.; Roy, S. L.; Tambe, M. A.; Rochet, J. C.; Galvagnion, C.; Skibinski, G.; Finkbeiner, S.; Bova, M.; Regnstrom, K.; Chiou, S. S.; Johnston, J.; Callaway, K.; Anderson, J. P.; Jobling, M. F.; Buell, A. K.; Yednock, T. A.; Knowles, T. P.; Vendruscolo, M.; Christodoulou, J.; Dobson, C. M.; Schenk, D.; McConlogue, L., Targeting the intrinsically disordered structural ensemble of alpha-synuclein by small molecules as a potential therapeutic strategy for Parkinson's disease. *PLoS One* **2014**, *9* (2), e87133.
13. Zhu, M.; De Simone, A.; Schenk, D.; Toth, G.; Dobson, C. M.; Vendruscolo, M., Identification of small-molecule binding pockets in the soluble monomeric form of the Abeta42 peptide. *J Chem Phys* **2013**, *139* (3), 035101.
14. Zhang, Y.; Cao, H.; Liu, Z., Binding cavities and druggability of intrinsically disordered proteins. *Protein Sci* **2015**, *24* (5), 688-705.
15. Mollica, L.; Bessa, L. M.; Hanouille, X.; Jensen, M. R.; Blackledge, M.; Schneider, R., Binding Mechanisms of Intrinsically Disordered Proteins: Theory, Simulation, and Experiment. *Front Mol Biosci* **2016**, *3*, 52.
16. Yu, C.; Niu, X.; Jin, F.; Liu, Z.; Jin, C.; Lai, L., Structure-based Inhibitor Design for the Intrinsically Disordered Protein c-Myc. *Sci Rep* **2016**, *6*, 22298.

17. Larbig, G.; Pickhardt, M.; Lloyd, D. G.; Schmidt, B.; Mandelkow, E., Screening for inhibitors of tau protein aggregation into Alzheimer paired helical filaments: a ligand based approach results in successful scaffold hopping. *Curr Alzheimer Res* **2007**, *4* (3), 315-23.
18. Bulic, B.; Pickhardt, M.; Schmidt, B.; Mandelkow, E. M.; Waldmann, H.; Mandelkow, E., Development of tau aggregation inhibitors for Alzheimer's disease. *Angew Chem Int Ed Engl* **2009**, *48* (10), 1740-52.
19. Tomasic, T.; Peterlin Masic, L., Rhodanine as a scaffold in drug discovery: a critical review of its biological activities and mechanisms of target modulation. *Expert Opin Drug Discov* **2012**, *7* (7), 549-60.
20. JW, M. N.; Blackburn, S., Quantification of frequent-hitter behavior based on historical high-throughput screening data. *Future Med Chem* **2014**, *6* (10), 1113-26.
21. Baell, J. B.; Holloway, G. A., New substructure filters for removal of pan assay interference compounds (PAINS) from screening libraries and for their exclusion in bioassays. *J Med Chem* **2010**, *53* (7), 2719-40.
22. Pickhardt, M.; Neumann, T.; Schwizer, D.; Callaway, K.; Vendruscolo, M.; Schenk, D.; St George-Hyslop, P.; Mandelkow, E. M.; Dobson, C. M.; McConlogue, L.; Mandelkow, E.; Toth, G., Identification of Small Molecule Inhibitors of Tau Aggregation by Targeting Monomeric Tau As a Potential Therapeutic Approach for Tauopathies. *Curr Alzheimer Res* **2015**, *12* (9), 814-28.
23. Pickhardt, M.; Biernat, J.; Hubschmann, S.; Dennissen, F. J. A.; Timm, T.; Aho, A.; Mandelkow, E. M.; Mandelkow, E., Time course of Tau toxicity and pharmacologic prevention in a cell model of Tauopathy. *Neurobiol Aging* **2017**, *57*, 47-63.
24. Schirmer, R. H.; Adler, H.; Pickhardt, M.; Mandelkow, E., "Lest we forget you--methylene blue...". *Neurobiol Aging* **2011**, *32* (12), 2325 e7-16.
25. Wischik, C. M.; Edwards, P. C.; Lai, R. Y.; Roth, M.; Harrington, C. R., Selective inhibition of Alzheimer disease-like tau aggregation by phenothiazines. *Proc Natl Acad Sci U S A* **1996**, *93* (20), 11213-8.
26. Taniguchi, S.; Suzuki, N.; Masuda, M.; Hisanaga, S.; Iwatsubo, T.; Goedert, M.; Hasegawa, M., Inhibition of heparin-induced tau filament formation by phenothiazines, polyphenols, and porphyrins. *J Biol Chem* **2005**, *280* (9), 7614-23.
27. Crowe, A.; James, M. J.; Lee, V. M.; Smith, A. B., 3rd; Trojanowski, J. Q.; Ballatore, C.; Brunden, K. R., Aminothienopyridazines and methylene blue affect Tau fibrillization via cysteine oxidation. *J Biol Chem* **2013**, *288* (16), 11024-37.
28. Akoury, E.; Pickhardt, M.; Gajda, M.; Biernat, J.; Mandelkow, E.; Zweckstetter, M., Mechanistic basis of phenothiazine-driven inhibition of Tau aggregation. *Angew Chem Int Ed Engl* **2013**, *52* (12), 3511-5.
29. Pakavathkumar, P.; Sharma, G.; Kaushal, V.; Foveau, B.; LeBlanc, A. C., Methylene Blue Inhibits Caspases by Oxidation of the Catalytic Cysteine. *Sci Rep* **2015**, *5*, 13730.
30. Stack, C.; Jainuddin, S.; Elipenahli, C.; Gerges, M.; Starkova, N.; Starkov, A. A.; Jove, M.; Portero-Otin, M.; Launay, N.; Pujol, A.; Kaidery, N. A.; Thomas, B.; Tampellini, D.; Beal, M. F.; Dumont, M., Methylene blue upregulates Nrf2/ARE genes and prevents tau-related neurotoxicity. *Hum Mol Genet* **2014**, *23* (14), 3716-32.
31. Hochgrafe, K.; Sydow, A.; Matenia, D.; Cadinu, D.; Konen, S.; Petrova, O.; Pickhardt, M.; Goll, P.; Morellini, F.; Mandelkow, E.; Mandelkow, E. M., Preventive methylene blue treatment preserves cognition in mice expressing full-length pro-aggregant human Tau. *Acta Neuropathol Commun* **2015**, *3*, 25.
32. Yao, T. M.; Tomoo, K.; Ishida, T.; Hasegawa, H.; Sasaki, M.; Taniguchi, T., Aggregation analysis of the microtubule binding domain in tau protein by spectroscopic methods. *J Biochem* **2003**, *134* (1), 91-9.
33. von Bergen, M.; Friedhoff, P.; Biernat, J.; Heberle, J.; Mandelkow, E. M.; Mandelkow, E., Assembly of tau protein into Alzheimer paired helical filaments depends on a local sequence

- motif ((306)VQIVYK(311)) forming beta structure. *Proc Natl Acad Sci U S A* **2000**, *97* (10), 5129-34.
34. Barghorn, S.; Biernat, J.; Mandelkow, E., Purification of recombinant tau protein and preparation of Alzheimer-paired helical filaments in vitro. *Methods Mol Biol* **2005**, *299*, 35-51.
35. Kadavath, H.; Jaremko, M.; Jaremko, L.; Biernat, J.; Mandelkow, E.; Zweckstetter, M., Folding of the Tau Protein on Microtubules. *Angew Chem Int Ed Engl* **2015**, *54* (35), 10347-51.
36. Kozakov, D.; Grove, L. E.; Hall, D. R.; Bohnuud, T.; Mottarella, S. E.; Luo, L.; Xia, B.; Beglov, D.; Vajda, S., The FTMap family of web servers for determining and characterizing ligand-binding hot spots of proteins. *Nat Protoc* **2015**, *10* (5), 733-55.
37. Flanagan, M. E.; Abramite, J. A.; Anderson, D. P.; Aulabaugh, A.; Dahal, U. P.; Gilbert, A. M.; Li, C.; Montgomery, J.; Oppenheimer, S. R.; Ryder, T.; Schuff, B. P.; Uccello, D. P.; Walker, G. S.; Wu, Y.; Brown, M. F.; Chen, J. M.; Hayward, M. M.; Noe, M. C.; Obach, R. S.; Philippe, L.; Shanmugasundaram, V.; Shapiro, M. J.; Starr, J.; Stroh, J.; Che, Y., Chemical and computational methods for the characterization of covalent reactive groups for the prospective design of irreversible inhibitors. *J Med Chem* **2014**, *57* (23), 10072-9.
38. Sormanni, P.; Piovesan, D.; Heller, G. T.; Bonomi, M.; Kukic, P.; Camilloni, C.; Fuxreiter, M.; Dosztanyi, Z.; Pappu, R. V.; Babu, M. M.; Longhi, S.; Tompa, P.; Dunker, A. K.; Uversky, V. N.; Tosatto, S. C.; Vendruscolo, M., Simultaneous quantification of protein order and disorder. *Nat Chem Biol* **2017**, *13* (4), 339-342.
39. Varadi, M.; Kosol, S.; Lebrun, P.; Valentini, E.; Blackledge, M.; Dunker, A. K.; Felli, I. C.; Forman-Kay, J. D.; Kriwacki, R. W.; Pierattelli, R.; Sussman, J.; Svergun, D. I.; Uversky, V. N.; Vendruscolo, M.; Wishart, D.; Wright, P. E.; Tompa, P., pE-DB: a database of structural ensembles of intrinsically disordered and of unfolded proteins. *Nucleic Acids Res* **2014**, *42* (Database issue), D326-35.
40. Schrödinger, *Release 2016-1*, Schrödinger, New York, NY, USA, 2016.
41. Miao, Z.; Cao, Y.; Jiang, T., RASP: rapid modeling of protein side chain conformations. *Bioinformatics* **2011**, *27* (22), 3117-22.
42. Touw, W. G.; Baakman, C.; Black, J.; te Beek, T. A.; Krieger, E.; Joosten, R. P.; Vriend, G., A series of PDB-related databanks for everyday needs. *Nucleic Acids Res* **2015**, *43* (Database issue), D364-8.
43. Kozakov, D.; Hall, D. R.; Chuang, G. Y.; Cencic, R.; Brenke, R.; Grove, L. E.; Beglov, D.; Pelletier, J.; Whitty, A.; Vajda, S., Structural conservation of druggable hot spots in protein-protein interfaces. *Proc Natl Acad Sci U S A* **2011**, *108* (33), 13528-33.
44. *OMEGA 2.5.1.4*, OpenEye Scientific Software: Santa Fe, NM, USA, <http://www.eyesopen.com>
45. Hawkins, P. C.; Skillman, A. G.; Warren, G. L.; Ellingson, B. A.; Stahl, M. T., Conformer generation with OMEGA: algorithm and validation using high quality structures from the Protein Databank and Cambridge Structural Database. *J Chem Inf Model* **2010**, *50* (4), 572-84.
46. *QUACPAC 1.6.3*; OpenEye Scientific Software: Santa Fe, NM, USA, <http://www.eyesopen.com>
47. McGann, M., FRED and HYBRID docking performance on standardized datasets. *J Comput Aided Mol Des* **2012**, *26* (8), 897-906.
48. McGann, M., FRED pose prediction and virtual screening accuracy. *J Chem Inf Model* **2011**, *51* (3), 578-96.
49. Kelley, B. P.; Brown, S. P.; Warren, G. L.; Muchmore, S. W., POSIT: Flexible Shape-Guided Docking For Pose Prediction. *J Chem Inf Model* **2015**, *55* (8), 1771-80.
50. *OEDOCKING 3.2.0.2*; OpenEye Scientific Software: Santa Fe, NM, USA, <http://www.eyesopen.com>
51. *FRED, 2.2.5*: OpenEye Scientific Software: Santa Fe, NM, USA <http://www.eyesopen.com>
52. Barghorn, S.; Zheng-Fischhofer, Q.; Ackmann, M.; Biernat, J.; von Bergen, M.; Mandelkow, E. M.; Mandelkow, E., Structure, microtubule interactions, and paired helical filament aggregation by tau mutants of frontotemporal dementias. *Biochemistry* **2000**, *39* (38), 11714-21.
53. *XLSTAT 19.4.*; , Addinsoft: Paris, France, 2017.

1
2
3
4
5
6
7
8
9
10
11
12
13
14
15
16
17
18
19
20
21
22
23
24
25
26
27
28
29
30
31
32
33
34
35
36
37
38
39
40
41
42
43
44
45
46
47
48
49
50
51
52
53
54
55
56
57
58
59
60

Table of Contents Graphic

